Chapter 2

Photosensitivity and Photosensitization of Optical Fibers

We have seen in the last chapter that optical fibers have very good optical properties for light transmission. Electronic absorptions that lead to attenuation are in the deep UV wavelength regime, and the molecular vibrations are far removed from the optical fiber transmission windows of interest to telecommunications. We have briefly considered the possible link between the change in absorption and the effect on the refractive index. Another possibility for the refractive index change is via an electro-optic nonlinearity. However, the symmetry properties of glass prohibit the electro-optic effect [1]. If there is an electro-optic contribution to the changes in the refractive index as a result of exposure to UV radiation, then an internal order would have to be created. This chapter considers aspects of defects connected with photosensitivity and techniques for photosensitization of optical fibers. We briefly compare in Section 2.1 the electro-optic effect [2] and how this may be invoked in glass. This aspect has recently received considerable interest worldwide but, as already stated, will not be studied in this book in any detail. Section 2.2 introduces some of the defects that are linked to the UV-induced change in refractive index of glass. The hot debate on defects has continued for a number of years and there are a vast number of "subtleties" with regards to the same nominal defect state, as well as pathways to achieving transformations from one state to the other. Some of the defects cannot be detected

by optical means and require sophisticated methods. The task is not made easy by the various nomenclature used in labeling, so that unraveling defects is made inaccessible to the layman. A simple *overview* of the important defects is given and we point to the literature for a detailed discussion [3,4]. Section 2.3 looks at the evidence of photoexcitation of electrons and, in conjunction with Section 2.2, the methods for the detection of defects. The routes used to photosensitize and fabricate fibers are presented in the last section.

2.1 Photorefractivity and photosensitivity

It is useful to distinguish the term *photorefractivity* from photosensitivity and photochromic effect. Photorefractivity refers to a phenomenon usually ascribed to crystalline materials that exhibit a second-order nonlinearity by which light radiation can change the refractive index by creating an internal electric field [5]. Photosensitivity invariably refers to a permanent change in refractive index or opacity induced by exposure to light radiation with the internal field playing an insignificant role. The term traditionally applies to the color change in certain glasses with exposure to ultraviolet radiation and heat. Photochromic glass does not depend on the application of heat to change opacity, and the action is reversible. However, a combination of these properties is possible in glasses and is a novel phenomenon, which is currently being studied, not least because it is poorly understood. Considering the normal polarization response of materials to applied electric fields may provide a physical insight into the phenomenon of photorefractivity and poling of glass.

The induced polarization, P, in a medium can be described by the relationship

$$D = \varepsilon_0 E + P, \tag{2.1.1}$$

where D is the displacement, E is the applied field, ε_0 is the free space permittivity, and P is the induced polarization. In a material in which the polarization is nonlinear, the polarization may be expanded in powers of the applied field as

$$\begin{aligned} P &= \varepsilon_0 \chi^{(1)} E + \varepsilon_0 \chi^{(2)} E^2 + \varepsilon_0 \chi^{(3)} E^3 + \ldots \\ &= \varepsilon_0 \{\chi^{(1)} E + \chi^{(2)} E^2 + \chi^{(3)} E^3 + \ldots\} \end{aligned} \tag{2.1.2}$$

and

$$\varepsilon_r = \frac{D}{\varepsilon_0 E} = 1 + \chi^{(1)}, \tag{2.1.3}$$

where $\varepsilon_r = 1 + \chi^{(1)}$ is the linear permittivity, $\chi^{(2)}$ is the first term of the nonlinear susceptibility (which can be nonzero in crystalline media), and $\chi^{(3)}$ is the third-order nonlinearity (nonzero in all materials).

Using Equations (2.1.2) and (2.1.3), the perturbed permittivity under the influence of an applied electric field is

$$\frac{D}{\varepsilon_0 E} = \varepsilon_r + \chi^{(2)}E + \chi^{(3)}E^2 \ldots \tag{2.1.4}$$

$$= \varepsilon_r + \Delta\varepsilon = \varepsilon, \tag{2.1.5}$$

and since the refractive index n is related to the permittivity as

$$\begin{aligned} \varepsilon &= n^2 \\ &= (n_0 + \Delta n)^2, \\ &\approx n_0^2 + 2n_0\Delta n \end{aligned} \tag{2.1.6}$$

from which immediately follows

$$\Delta n = \frac{1}{2n_0}[\chi^{(2)}E + \chi^{(3)}E^2 \ldots]. \tag{2.1.7}$$

In photorefractive materials with an active $\chi^{(2)}$, an internal charge can build up due to trapped carriers released from defects. These give rise to an internal field, which modulates the refractive index locally via the first term in Eq. (2.1.7). The induced index changes result directly from the linear electro-optic effect ($\chi^{(2)}$) and are in general quite large, $\sim 10^{-4}$. However, with $\chi^{(2)}$ being zero in glass, the induced refractive index with an applied field can only result from the nonzero third-order susceptibility, $\chi^{(3)}$. Even if an internal field could develop, the refractive index change is small, $\sim 10^{-7}$; however, as will be seen, if an internal field is possible in glass, it results in a modest nonlinearity [2]. We now assume the existence of an internal field E_{dc} and apply an external field $E_{applied}$. The induced index change is as follows:

$$\Delta n = \frac{1}{2n_0}\chi^{(3)}(E_{dc} + E_{applied})^2 \tag{2.1.8}$$

$$= n_2'(E_{dc}^2 + 2E_{dc} \times E_{applied} + E_{applied}^2). \tag{2.1.9}$$

The first term in Eq. (2.1.9) indicates a permanent index change, whereas the third term is the usual quadratic nonlinear effect known as the dc-Kerr effect. We have used a prime on the n_2', to distinguish it from the optical Kerr constant n_2. The interesting relationship is described by the remaining term,

$$\Delta n = 2n_2' E_{dc} \times E_{applied}. \tag{2.1.10}$$

This relationship is analogous to the linear electro-optic effect, in which the applied field operates on an enhanced nonlinearity, $2n_2' E_{dc}$, due to the frozen internal field. If the internal field is large, then a useful nonlinearity is possible. This effect is believed to be partly the basis of poled glass [2].

In crystalline media with a large photorefractive response, the nonlinearity $\chi^{(2)}$ is several orders of magnitude larger than the next higher order coefficient, $\chi^{(3)}$ (and hence n_2') in glass. From the first term in Eq. (2.1.9) we can calculate the required field for a change in the refractive index of 10^{-3}. With a measured value of $\chi^{(3)} \sim 10^{-22}\,\mathrm{m^{-2}V^{-2}}$ for silica, a large internal field of $\sim 10^9$ V/m would be necessary, equivalent to n_2' of ~ 1 pm $\mathrm{V^{-1}}$. These values have been exceeded in UV photoelectrically *poled* fiber, with the highest reported result of ~6 pm/V [6]! Combined with the low dielectric constant of silica, it has a potentially large bandwidth for electro-optic modulation. Just how such a large field may develop has been debated. However, it has been suggested by Myers *et al.* [7,8] that the poling voltage is dropped across a thin layer (~5 μm) within the glass, causing huge fields to appear.

The electro-optic nature of UV photoinduced refractive index in Bragg gratings has not been reported, although the presence charges related to defects could indeed develop an internal field, as in the case of second-harmonic generation in glass [9]. In the next section, we consider some of the important defects, which are of interest in unraveling the mystery of photosensitivity of glass.

2.2 Defects in glass

The nature of fabrication of glass is ideally suited to promoting defects. The chemical reactions that take place in a modified chemical vapor deposition (MCVD) [10] process are based on hot gases reacting to form a soot deposit on the inside of a silica support tube or on the outside in outside vapor phase deposition (OVD). The process allows the ratio of reactive gases such as silicon/germanium tetrachloride and oxygen to be

easily changed to arrive at a nearly complete chemical reaction, depositing a mixture of germanium and silicon dioxides. It is not possible to have a 100% reaction, so the deposited chemicals have a proportion of suboxides and defects within the glass matrix. With sintering and preform collapse, these reaction components remain, although further alterations may take place while the fiber is being drawn, when bonds can break [11–13]. The end result is a material that is highly inhomogeneous on a microscopic scale with little or no order beyond the range of a few molecular distances. The fabrication process also allows other higher-order ring structures [14] to form, complicating the picture yet further. There is a possibility of incorporating not only a strained structure, but also one which has randomly distributed broken bonds and trapped defects.

This is especially true of a fiber with the core dopant germanium, which readily forms suboxides as GeO_x (x = 1 to 4), creating a range of defects in the tetrahedral matrix of the silica host glass. Given this rich environment of imperfection, it is surprising that state-of-the-art germania-doped silica fiber has extremely good properties—low loss and high optical damage threshold—and is a result of better understanding of defects, which lead to increased attenuation in the transmission windows of interest.

Among the well-known defects formed in the germania-doped silica core are the paramagnetic Ge(n) defects, where n refers to the number of next-nearest-neighbor Ge/Si atoms surrounding a germanium ion with an associated unsatisfied single electron, first pointed out by Friebele *et al.* [17]. These defects are shown schematically in Fig. 2.1. The Ge(1) and Ge(2) have been identified as trapped-electron centers [18]. The GeE′, previously known as the Ge(0) and the Ge(3) centers, which is common in oxygen-deficient germania, is a hole trapped next to a germanium at an oxygen vacancy [19] and has been shown to be independent of the number of next-neighbor Ge sites. Here an oxygen atom is missing from the tetrahedron, while the germania atom has an extra electron as a dangling bond. The extra electron distorts the molecule of germania as shown in Fig. 2.2.

The GeO defect, shown in Fig. 2.2 (LHS), has a germanium atom coordinated with another Si or Ge atom. This bond has the characteristic 240-nm absorption peak that is observed in many germanium-doped photosensitive optical fibers [21]. On UV illumination, the bond readily breaks, creating the GeE′ center. It is thought that the electron from the GeE′ center is liberated and is free to move within the glass matrix via hopping or tunneling, or by two-photon excitation into the conduction

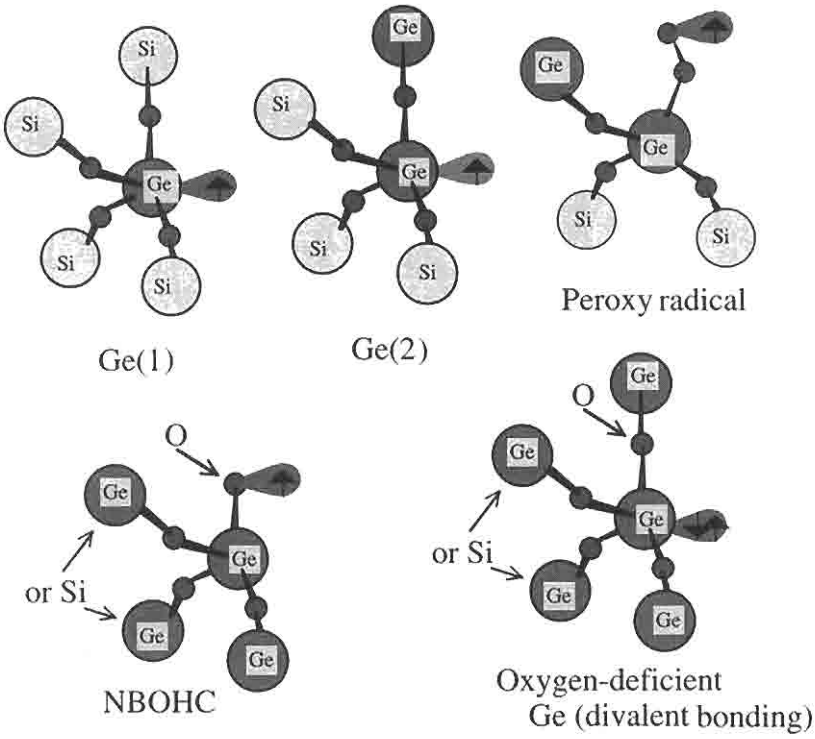

Figure 2.1: A schematic of proposed Ge (or Si) defects of germania-doped silica. The characteristic absorption of the Ge(1) is ~280 nm (4.4 eV) [18] and is a trapped electron at a Ge (or Si) site; Ge(2) has an absorption at 213 nm (5.8 eV) and is a hole center. The peroxy radical has an absorption at 7.6 eV (163 nm) and at 325 nm (3.8 eV) [15,16].

band [22–24]. This electron can be retrapped at the original site or at some other defect site. The removal of this electron, it is believed, causes a reconfiguration of the shape of the molecule (see Fig. 2.2), possibly also changing the density of the material, as well as the absorption. It appears that the Ge(1) center is the equivalent of the germanium defects observed in α-quartz, known as the Ge(I) and Ge(II), but less well defined [23].

Phosphorus forms a series of defects similar to those of germanium. However, the photosensitivity is limited at 240 nm and requires shorter wavelengths, such as 193-nm radiation [24].

Other defects include the nonbridging oxygen hole center (NBOHC), which is claimed to have absorptions at 260 and 600 nm, and the peroxy

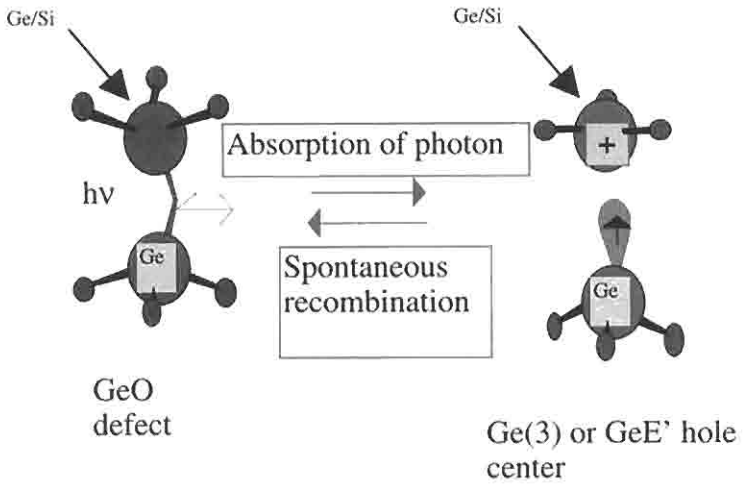

Figure 2.2: The GeO defect of germania-doped silica, in which the atom adjacent to germanium is either a silicon or another germanium. It can absorb a photon to form a GeE′ defect. The Ge(0) or Ge(3) are a GeE′ center [20]. The GeE′ defect shows the extra electron (associated with the Ge atom), which may be free to move within the glass matrix until it is retrapped at the original defect site, at another GeE′ hole site, or at any one of the Ge(n) defect centers.

radical (P-OHC) [25], believed to absorb at 260 nm. Both are shown in Fig. 2.1.

2.3 Detection of defects

A considerable amount of work has been done in understanding defects in glass. Detection of defects may be broadly categorized into four groups: optically active defects can be observed because of their excitation spectrum or excitation and luminescence/fluorescence spectrum while optically inactive defects are detectable by their electron spin resonance signature, or ESR spectrum, together with optical emission spectrum.

The model of the defects as shown in Fig. 2.2 suggests the liberation of electrons on absorption of UV radiation. It should therefore be possible to detect liberated charges experimentally; since silica has a high volume resistivity, it is necessary to choose a geometry that can directly enable the measurement of electric currents. Photosensitivity has been explored

both indirectly, e.g., by etching glass exposed to radiation or using second-harmonic generation [9,26,27] as a probe, and directly, e.g., by measurement of photocurrent in germania-doped planar waveguides [28] and across thin films of bulk glass [29].

It has been concluded that the photocurrent is influenced by the fluence of the exciting UV radiation; the photocurrent (probably by tunneling [29]) is a linear function of the power density for CW excitation [28], while for pulsed, high-intensity radiation, it takes on a two-photon excitation characteristic [29].

The paramagnetic defects of the Ge(n) type including the E′ center are detected by ESR. The GeE′ has an associated optical absorption at 4.6 eV [30].

2.4 Photosensitization techniques

A question often asked is: Which is the best fiber to use for the fabrication of most gratings? Undoubtedly, the preferred answer to this question should be standard telecommunications fiber. Although techniques have been found to write strong gratings in this type of fiber, there are several reasons why standard fiber is not the best choice for a number of applications. Ideally, a compatibility with standard fiber is desirable, but the design of different devices requires a variety of fibers. This does open the possibility of exploiting various techniques for fabrication and sensitization. Here we look in some detail at the behavior of commonly used species in optical fiber and present their properties, which may influence the type of application. For example, the time or intensity of UV exposure required for the writing of gratings affects the transmission and reliability properties. This results in either damage (Type II gratings) [31] or the formation of Type I, at low fluence, and Type IIA gratings [32], each of which have different characteristics (see Section 2.4.1).

The use of boron and tin as a codopant in germanosilicate fibers, hot hydrogenation and cold, high-pressure hydrogenation, and flame-assisted low-pressure hydrogenation ("flame-brushing") are well-established photosensitization methods. The type of the fiber often dictates what type of grating may be fabricated, since the outcome depends on the dopants.

The literature available on the subjects of photosensitivity, the complex nature of defects, and the dynamics of growth of gratings is vast

[34]. The sheer numbers of different fibers available worldwide, further complicates the picture and by the very nature of the limited fiber set available within the framework of a given study and the complex nature of glass, comparisons have been extremely difficult to interpret. This is not a criticism of the research in this field, merely a statement reiterating the dilemma facing researchers: how to deal with far too many variables! In order to draw conclusions from the available data, one can simply suggest a trend for the user to follow. A choice may be made from the set of commonly available fibers. For a certain set of these fibers (e.g., standard telecommunications fiber) the method for photosensitization may be simply hydrogenation, or 193-nm exposure. It is often the availability of the laser source that dictates the approach.

2.4.1 Germanium-doped silica fibers

Photosensitivity of optical fibers has been correlated with the concentration of GeO defects in the core [33,34]. The presence of the defect is indicated by the absorption at 240 nm, first observed by Cohen and Smith [35] and attributed to the reduced germania state, Ge(II). The number of these defects generally increases as a function of Ge concentration. Figure 2.3 shows the absorption at 242 nm in a perform with the germa-

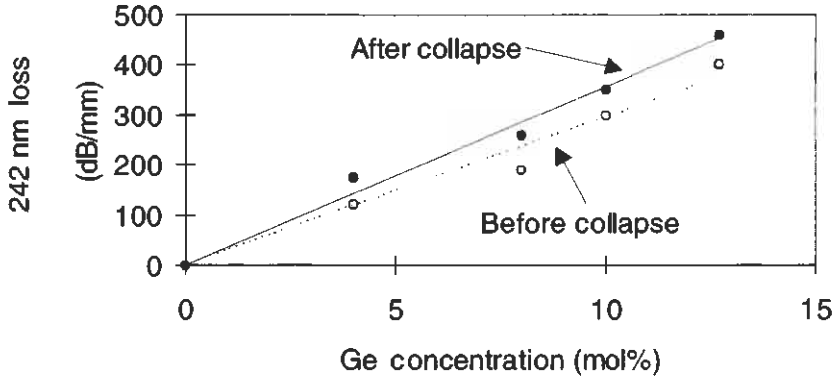

Figure 2.3: Absorption at 242 nm in preform samples before and after collapse as a function of Ge concentration (after Ref. [36]).

nium concentration [36]. The slope in this graph is ~28 dB/(mm-mol%) of Ge before the preform sample is collapsed (dashed line). After collapse, the number of defects increases, and the corresponding absorption changes to ~36 dB/(mm-mol%) (Fig. 2.3 continuous line).

Increasing the concentration of defects increases the photosensitivity of the fiber. This can be done by collapsing the fiber in a reducing atmosphere, for example, by replacing oxygen with nitrogen or helium [36] or with hydrogen [37,49].

The 240-nm absorption peak is due to the oxygen-deficient hole center defect, (Ge-ODHC) [38] and indicates the intrinsic photosensitivity. It can be quantified as [39]

$$k = \alpha_{242\ \mathrm{nm}}/C, \tag{2.4.1}$$

where $\alpha_{242\ \mathrm{nm}}$ is the absorption at 242 nm and C is the molar concentration of GeO_2. Normally C lies between 10 and 40 dB/(mm-mol% GeO_2). Hot hydrogenation is performed on fibers or preforms at a temperature of ~650°C for 200 hours is 1 atm hydrogen [40]. The absorption at 240 nm closely follows the profile of the Ge concentration in the fiber [33], and k has been estimated to be large, ~120 dB/(mm-mol% GeO_2).

The saturated UV-induced index change increases approximately linearly with Ge concentration after exposure to UV radiation, from $\sim 3 \times 10^{-5}$ (3 mol% $GeO\%_2$) for standard fiber to $\sim 2.5 \times 10^{-4}$ (~20 mol% GeO_2) concentration, using a CW laser source operating at 244 nm [49]. However, the picture is more complex than the observations based simply on the use of CW lasers. With pulsed laser sources, high-germania-doped fiber (8%) shows an the initial growth rate of the UV-induced refractive index change, which is proportional to the energy density of the pulse. For low germania content, as in standard telecommunications fiber, it is proportional to the square of the energy density. Thus, two-photon absorption from 193 nm plays a crucial role in inducing maximum refractive index changes as high as ~0.001 in standard optical fibers [41]. Another, more complex phenomenon occurs in untreated germania fibers with long exposure time, in conjunction with both CW and pulsed radiation, readily observable in high germania content fibers [47]. In high-germania fiber, long exposure erases the initial first-order grating completely, while a second-order grating forms. This erasure of the first-order and the onset of second-order gratings forms a demarcation between Type I and Type IIA gratings.

Increasing the energy density damages the fiber core, forming Type II gratings [31]. The thermal history of the fiber is also of great importance, as is the mechanical strain during the time of grating inscription. Significantly, even strains as low as 0.2% can increase the peak refractive index modulation of the Type IIA grating in high germanium content fiber [42,43]. High-germania-doped (30%Ge) fibers drawn under high pulling tension show the opposite behavior [44], indicating the influence of elastic stress during drawing rather than the effect of drawing-induced defects [45]. Annealing the fiber at 1100°C for 1 hour and then cooling over 2 days reduces the time for the erasure of the Type I grating, as well as increasing the maximum refractive index modulation achievable in the Type IIA regime. With tin as a codopant in high-germanium fiber, the general overall picture changes slightly, but the dynamics are similar, except for reduced index change under strained inscription [46]. Thus, absolute comparison is difficult, and one may use the germania content as an indicator, bearing in mind the complex nature of the dynamics of grating formation in germania-doped silica fiber. Typical results for a high-germania fiber are shown in Fig. 2.4. The growth of the refractive index modulation as a function of time stops in the case of all three fibers shown, dropping to zero before increasing once again to form Type IIA gratings.

Photosensitivity of fiber fabricated under reduced conditions as a function Ge concentration also increases, but it is not sufficient to interpret the data by the maximum index change. The reason for this is the induction of Type IIA gratings [47] in relatively low concentration of Ge. Measurements performed under pulsed conditions reveal that the onset of the Type IIA grating is almost certainly always possible in any concentration of Ge; only the time of observation increases with low concentrations, although for practical purposes this time may be too long to be of concern. Figure 2.5 shows data from the growth of the average index on UV exposure as a function of Ge concentration in fibers, which have been reduced. The maximum index should change monotonically; however, above a certain concentration, the onset of Type IIA forces the observed maximum index change for point B (20 mol% Ge), since the grating being written slowly disappears before growing again. While the maximum reflectivity should increase to higher levels, within the time frame of the measurements this fiber appears to be less sensitive. A better indicator is the initial growth rate of the index change, since Type IIA grating is not observed for some time into the measurements. Figure 2.5 shows an

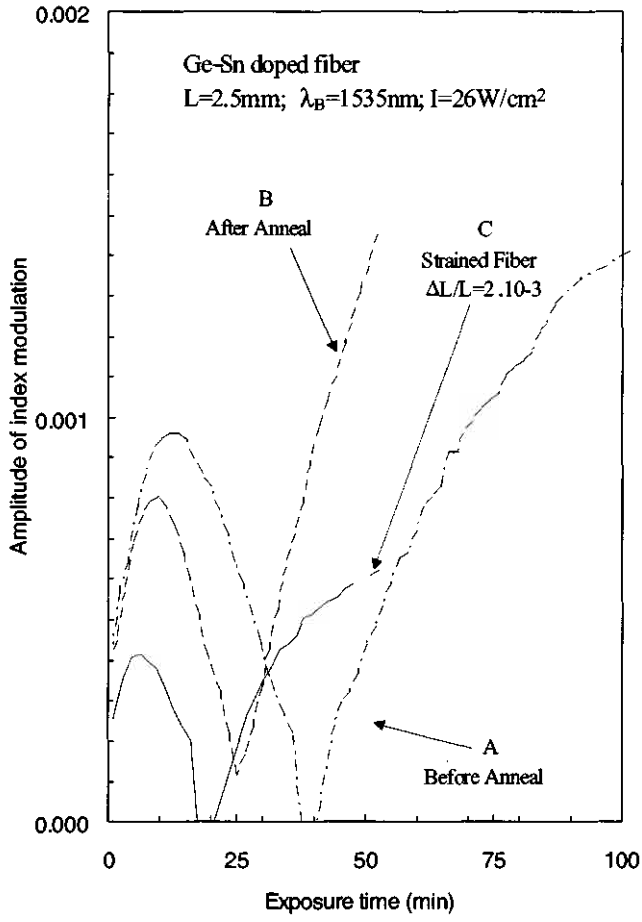

Figure 2.4: The growth dynamics of the refractive index change in 20 mol% Ge: 1 mol% Sn. The three data are for A: pristine fiber, B: after annealing, and C: under strain of 0.2%. The Type IIA grating begins after the initial erasure. (from: Douay M., Xie W. X., Taunay T., Bernage P., Niay P., Cordier P., Poumellec B., Dong L., Bayon J. F., Poignant H., and Delevaque E., "Densification involved in the UV based photosensitivity of silica glasses and optical fibers," *J. Lightwave Technol.* **15**(8), 1329–1342, 1997. © IEEE 1997.)

approximately linear increase in the rate of growth of the UV-induced average refractive index. The data has been interpreted from Ref. [48], bearing in mind that the for the initial growth rate in *low* germanium fibers, there is a time delay before the grating begins to grow.

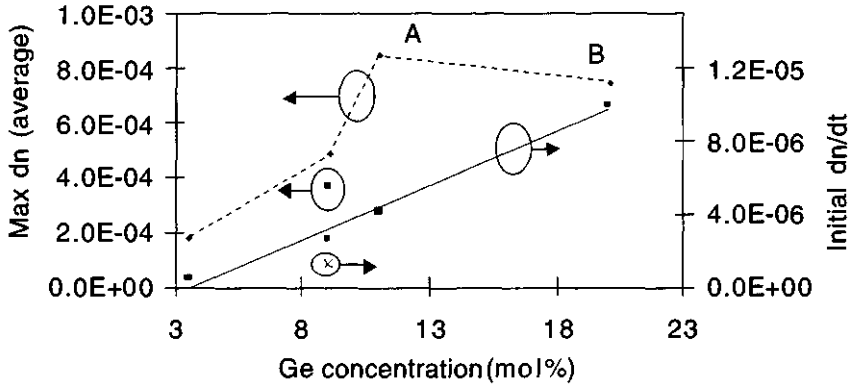

Figure 2.5: Concentration dependence of the maximum-index and its initial growth rate as a function of germania concentration in oxygen-deficient fibers. The two isolated points refer to unreduced samples (interpreted from Ref. [48]).

Figure 2.6 shows the actual growth of the transmission dip (equivalent to the increase in reflection) for several reduced germania fibers [48]. Note in particular the change in the transmission due to the onset of Type IIA grating. At this point, the Bragg wavelength shift is reduced [47], making the maximum average index measurement difficult.

Measurement of the shift in the Bragg wavelength is a reasonable indicator for the UV induced index change for a fiber well below the start of saturation effects. With saturation, care needs to be taken, since the bandwidth of the grating increases, making it more difficult to accurately measure the wavelength shift. The ac index change should be calculated from the bandwidth and the reflectivity data along with the Bragg wavelength shift to accurately gauge the overall ac and dc components of the index change (see Chapters 4 and 9).

The growth rate and the maximum index change are of interest if strong gratings are to be fabricated in a short time frame. This suggests that reduced germania is better than normal fiber on both counts. However, the maximum index change is still lower than required for a number of applications and the time of fabrication excessive. The use of hot hydrogen to reduce germania has the additional effect of increasing loss near 1390 nm due to the formation of OH^- hydroxyl ions [49,50]. The absorption loss at 1390 nm is estimated to be ~0.66, 0.5, and 0.25 dB/(m-mol%) at

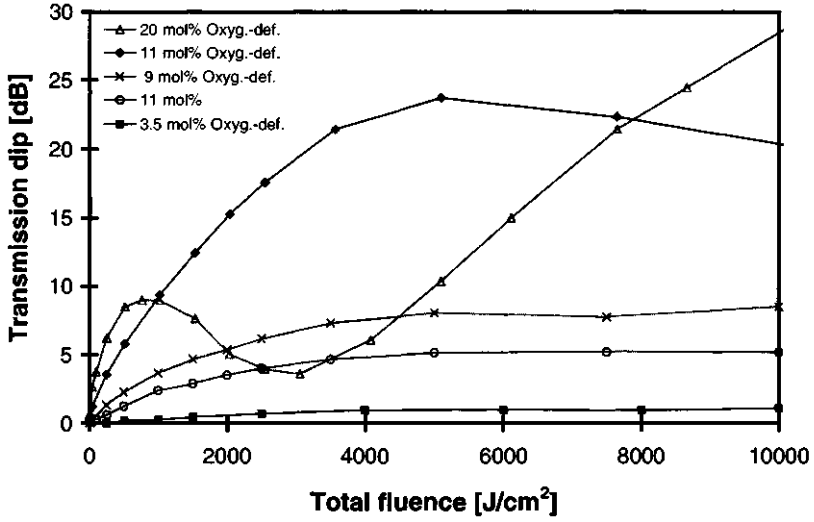

Figure 2.6: Growth of the transmission dip with fluence for different types of reduced germania fibers. For the 20 mol% germania fiber, a reduction in the reflectivity is probably due to Type IIA grating formation. (from: Grüner-Nielsen L. and Hübner J., "Photosensitive fiber for highly reflective Bragg gratings," in *Tech. Digest of Conf. on Opt. Fiber Commun. OFC'97,* paper WL16, p. 178, 1997.)

1390, 1500, and 1550 nm, respectively [40]. One major advantage of fibers that have been reduced is that they are rendered permanently photosensitive and require the minimum of processing, compared with hydrogenated fibers (see following sections).

The incorporation of 0.1% nitrogen in germanium-doped silica fiber by the surface plasma assisted chemical vapor deposition (SPCVD) process [51] has been shown to have a high photosensitivity [52]. The effect on the 240-nm absorption is dramatic, raising it to 100 dB/mm/mol% GeO_2, doubling it compared to the equivalent for germanium doping alone. The induced refractive index changes are reported to be large (2.8×10^{-3}) and much larger (0.01) with cold hydrogen soaking of 7 mol%Ge;0 mol%N fiber. The Type IIA threshold is reported to increase by a factor of ~6 over that in nitrogen-free, 20 mol% Ge fibers. However, there is evidence of increase in the absorption loss in the 1500-nm window with the addition of nitrogen. The next most photosensitive fibers are the germania–boron or tin-doped fibers.

2.4.2 Germanium–boron codoped silicate fibers

The use of boron in soda lime and silicate glass has been known for a long time [53]. It has also been established that boron, when added to germania-doped silicate glass, *reduces* the refractive index. The transformational changes that occur depend on the thermal history and processing of the glass. As such, it is generally used in the cladding of optical fibers, since the core region must remain at a higher refractive index. Compared to fluorine, the other commonly used element in the cladding (in conjunction with phosphorus), the refractive index modification is generally at least an order of magnitude larger, since more of the element can be incorporated in the glass. Thus, while the maximum index difference from fluorine can be approximately -10^{-3} with boron, the index change can be $>|-0.01|$. This opens up many possibilities for the fabrication of novel structures, not least as a component to allow the incorporation of even more germania into glass while keeping a low refractive index difference between the cladding and core when both are incorporated into the core. One advantage of such a composition is the fabrication of a fiber that is outwardly identical in terms of refractive index profile and core-to-cladding refractive index difference with standard single-mode optical fibers, and yet contains many times the quantity of germania in the core. The obvious advantage is the increased photosensitivity of such a fiber with the increased germania. Indeed, this is the case with boron–germanium (B-Ge) codoped fused silica fiber [54]. The typical profile of a B-Ge preform is shown Fig. 2.7. The raised refractive index dashed line shows the

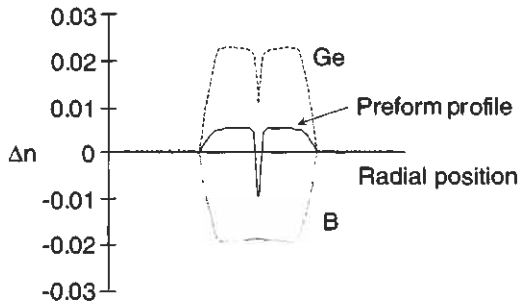

Figure 2.7: The refractive index components due to germanium and boron (dashed and dotted lines) contributing to the resultant preform profile (continuous line) [54].

contribution due to the germanium concentration, while the negative refractive contribution is due to the boron, resulting in the continuous line positive refractive index profile.

It should be noted that with boron and germanium, it is possible to selectively place a photosensitive region anywhere in the fiber, without altering the wave guiding properties. Other types of profiles possible are boron with highly doped germanium in a cladding matched to silica for liquid cored fibers [55], in-cladding gratings for lasers [56], and special fiber for side-tap filters and long-period gratings [57,58].

B-Ge codoped fiber is fabricated using MCVD techniques and a standard phosphorus–fluorine cladding matched silica tube with normal oxidizing conditions. The reactive precursor vapors are $SiCl_4$, BCl_3, and $GeCl_4$, with oxygen as a carrier for the core deposition. For a composition equivalent to ~16 mol% germanium, the photosensitivity in comparison with 20 mol% unreduced germanium fiber shows an improvement >3-fold in the UV-induced refractive index modulation as well as an order of magnitude reduction in the writing time. With respect to 10 mol% reduced germanium fiber, the improvement in the maximum refractive index modulation is ~40% with a ×6 reduction in the writing time. The maximum refractive index change is close to 10^{-3} for this fiber induced with a CW laser operating at 244 nm [54].

A point worth noting with B-Ge fibers is the increased stress, and consequently, increased induced birefringence [59]. The preforms are difficult to handle because of the high stress. However, the real advantages with B-Ge fibers are the shortened writing time, the larger UV-induced refractive index change, and, potentially, fibers that are compatible with any required profile, for small-core large NA fiber amplifiers, to standard fibers.

B-Ge fibers form Type IIA gratings [60] with a CW 244-nm laser, as is the case with the data shown in Fig. 2.4. This suggests that there is probably little difference due to the presence of boron; only the high germanium content is responsible for this type of grating. There is a possibility that stress is a contributing factor to the formation of Type IIA [61]; recent work does partially indicate this but for germanium-doped fibers [44].

Typically, gratings written with CW lasers in B-Ge fiber decay more rapidly than low germanium doped (5 mol%) fibers when exposed to heat. Gratings lose half their index modulation when annealed at ~400°C (B-Ge: 22:6.3 mol%) and ~650°C (Ge 5 mol%) [46] for 30 minutes. A detailed

study of the decay of gratings written in B-Ge may be found in Ref. [62]. The thermal annealing of gratings is discussed in Chapter 9.

Boron causes additional loss in the 1550-nm window, of the order of ~0.1 dB/m, which may not be desirable. For short gratings, this need not be of concern.

2.4.3 Tin–germanium codoped fibers

Fabrication of Sn codoped Ge is by the MCVD process used for silica fiber by incorporating $SnCl_4$ vapor. SnO_2 increases the refractive index of optical fibers and, used in conjunction with GeO_2, cannot be used as B_2O_3 to match the cladding refractive index, or to enhance the quantity of germanium in the core affecting the waveguide properties. However, it has three advantages over B-Ge fiber: The gratings survive a higher temperature, do not cause additional loss in the 1500-nm window, have a slightly increased UV-induced refractive index change, reported to be 3 times larger than that of B-Ge fibers. Compared with B-Ge, Sn-Ge fibers lose half the UV-induced refractive index change at ~600°C, similarly to standard fibers [63].

2.4.4 Cold, high-pressure hydrogenation

The presence of molecular hydrogen has been shown to increase the absorption loss in optical fibers over a period of time [64]. The field was studied extensively [65], and it is known that the hydrogen reacts with oxygen to form hydroxyl ions. The increase in the absorption at the first overtone of the OH vibration at a wavelength of 1.27 μm was clearly manifest by the broadband increase in loss in both the 1300-nm and, to a lesser extent, in the 1500-nm windows. Another effect of hydrogen is the reaction with the Ge ion to form GeH, considerably changing the band structure in the UV region. These changes, in turn, influence the local refractive index as per the Kramers–Kronig model. The reaction rates have been shown to be strongly temperature dependent [65]. It has been suggested that the chemical reactions are different on heat treatment and cause the formation of a different species compared to illumination with UV radiation. However, no noticeable increase in the 240-nm band is observed with the presence of interstitial molecular hydrogen in Ge-doped silica. The highest refractive index change induced by UV radiation is undoubtedly in cold hydrogen soaked germania fibers. As has been

seen, an atmosphere of hot hydrogen during the collapse process or hot hydrogen soaking of fibers enhances the GeO defect concentration [37]. The presence of molecular hydrogen has been known to induce increases in the absorption loss of optical fibers, since the early day of optical fibers [50]. Apart from being a nuisance in submarine systems, in which hydrogen seeps into the fiber, causing a loss that increases with time of exposure, cold high pressure hydrogen soaking has led to germanium-doped fibers with the highest observed photosensitivity [66]. Any germania-doped fiber may be made photosensitive by soaking it under high pressure (800 bar) and/or high temperature (<150°C). Molecular hydrogen in-diffuses to an equilibrium state. The process requires a suitable high-pressure chamber into which fibers may be left for hydrogen loading. Once the fiber is loaded, exposure to UV radiation is thought to lead to a dissociation of the molecule, leading to the formation of Si–OH and/or Ge–OH bonds. Along with this, there is formation of the Ge oxygen-deficient centers, leading to a refractive index change. Soaking the fiber at 200 bar at room temperature for ~2 weeks is sufficient to load the 125-micron diameter fiber at 21°C [66].

UV exposure of standard hydrogen fibers easily yields refractive index changes in excess of 0.011 [67] in standard telecommunications fiber, with a highest value of 0.03 inferred [68]. Almost all Ge atoms are involved in the reactions giving rise to the index changes. Figure 2.8 shows the changes in the refractive index profile of a standard fiber before and after exposure to pulsed UV radiation at 248 nm (~600 mJ/cm^2, 20 Hz, 60-minute exposure) [68]. The growth of gratings is long with CW lasers (duration of 20 minutes for strong gratings with refractive index changes of ~$1–2 \times 10^{-3}$). The picture is quite different with the growth kinetics when compared with non-hydrogen-loaded germania fibers. To date, Type IIA gratings have not been observed in hydrogen-loaded fibers. There is also no clear evidence of the stress dependence of grating growth [44]. Whereas in Type IIA the average UV-induced refractive index change is negative, in hydrogen-loaded fibers the average refractive index grows unbounded to large values (>0.01).

Heating a hydrogen-loaded fiber increases the refractive index rapidly, even in P_2O_5 and P_2O_5:Al_2O_3-doped multimode fibers [68], although pure silica is not sensitized.

The dynamic changes that occur in the process of fiber grating fabrication are complex. Even with hydrogen-loaded fibers, there are indications that as the grating grows, the absorption in the core increases in the UV,

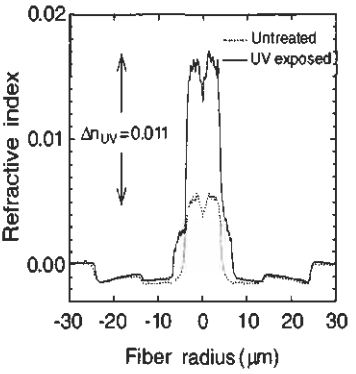

Figure 2.8: The refractive index profile of a 2.8% hydrogen-soaked standard fiber, before and after UV exposure with pulsed radiation at 248 nm (Courtesy P. Lemaire from: Lemaire P. J., Vengsarkar A. M., Reed W. A., and Mizarhi V., "Refractive index changes in optical fibers sensitized with molecular hydrogen," in *Technical Digest of Conf. on Opt. Fiber Commun., OFC'94,* pp. 47–48, 1994.)

as does the 400-nm luminescence [69]. Martin *et al.* [69] have found a direct correlation between refractive index change increase and luminescence. Figure 2.9 shows the transmission spectra of two gratings in hydrogenated standard fiber at different stages of growth, with the UV radiation at 244 nm CW switched on and off. With the UV switched on, the Bragg

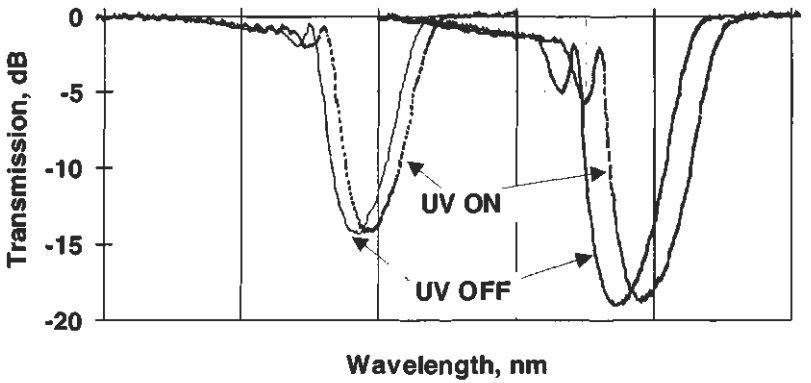

Figure 2.9: Shift in the Bragg wavelength as the UV radiation is switched on and off for two different strength gratings (after Ref. [70]).

wavelength shifts 0.05 nm to longer wavelengths at a grating reflectivity of ~1.4 dB. When the grating has grown to ~27 dB (different grating but same fiber), the shift is 0.1 nm, equivalent to an equilibrium temperature increase of the fiber of ~80°C. At the start of grating growth (<1 dB), the shift is not noticeable.

The formation of OH^- ions with UV exposure increases the loss in the 1500-nm window. There are two peaks associated with the formation of Si–OH (1.39 μm) and Ge–OH (1.42 μm) on UV exposure [71]. A concentration of 1 mol% of OH^- increases the loss at 1.4 μm by 5 dB. This is avoided by soaking the fiber in deuterium, which shifts the first overtone OD of the water peak to ~1.9 μm [74].

Another feature of hydrogen loading is the increased loss at wavelengths less than 1 μm after UV exposure of hydrogen-loaded fibers. The loss has a wavelength dependence at <0.95 μm of $e^{-4.6/\lambda}$, where λ is in microns [74].

Hydrogen loading of optical fibers

The loading of optical fibers with hydrogen is both temperature and pressure dependent. The diffusion coefficient of hydrogen is [50]

$$D = 2.83 \times 10^{-4} e^{(-40.19\ \text{kJ/mol})/RT},\ \text{cm}^2/\text{s}, \tag{2.4.2}$$

where $R = 8.311$ J/(K-mol) and T is the temperature in degrees Kelvin. The concentration of hydrogen in the fiber is calculated by solving the diffusion equation [72] as a function of radial position ρ and time t:

$$C(\rho,t) = \frac{2}{C_0} \sum_{n=1}^{\infty} \frac{J_0(\mu_n \rho)}{J_1^2(\mu_n \rho)} e^{-D(\mu_n/R)^2 t} \int_0^1 \varphi(\rho) J_0(\mu_n \rho) d\rho, \tag{2.4.3}$$

where μ_n are the nth zeroes of the J_0 Bessel function, D is the diffusion coefficient, and R is the radius of the fiber. C_0 is the initial concentration, and $\varphi(\rho) = 1$ if hydrogen is diffusing into the fiber and -1 for out-diffusion. The dynamics of the concentration have been modeled by Bhakti *et al.* [73] to study the effect on the drift of the resonance wavelength of a long-period grating. Under an ambient pressure of 200 bar, the in-diffusion of hydrogen is shown in Fig. 2.10 as a function of the radius of the radial position for different times. The out-diffusion of hydrogen is shown for different times as the fiber is removed from the high-pressure chamber [74] in Fig. 2.11. The first overtone OH^- peak at 1.245 μm can be used

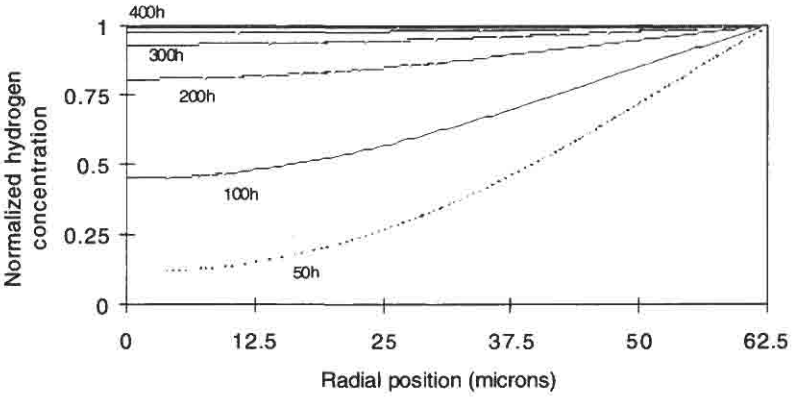

Figure 2.10: In-diffusion profile of hydrogen at 200 bar pressure in a 125-μm diameter fiber as a function of time at 23°C (courtesy F. Bhakti, Ref. [73]).

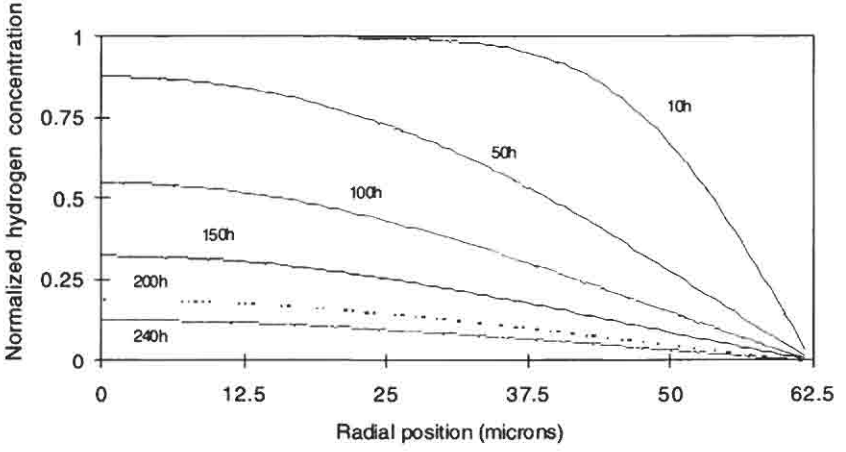

Figure 2.11: Out-diffusion profile of hydrogen in a 125-μm diameter fiber at 23°C (courtesy F. Bhakti, Ref. [73]).

to verify the concentration of hydrogen in the core [74,75]; the absorption at 1.245 μm is ~3 dB/(mol% H_2) (equivalent to 10^4 *ppm* in a mole of silica).

The wavelength shifts of long-period gratings (LPGs, see Chapter 4) resonances can be in excess of 150 nm to the long wavelength as the

hydrogen diffuses out of the core after fabrication of the grating, before returning to the original wavelength. Note that the resonance of the LPG is *only* dependent on the *difference* in the core and cladding refractive indexes, since it is the relative difference that is important (see Chapter 4). The effect on the refractive index of the fiber as the hydrogen out-diffuses is a complicated process, as shown by Malo *et al.* [76] using Bragg gratings. Once the fibers are removed from the chamber, the hydrogen begins to diffuse out but is fixed in the core by UV irradiation during grating fabrication. Depleted in the core, hydrogen in the cladding diffuses in before diffusing out. The stress changes the molecular polarizability of hydrogen [77], as well as the Bragg wavelength, first toward long, and then toward short wavelengths. The drift in the wavelength is found to be 0.72 nm for an initial pressure of 100 bar. The Bragg wavelength is sensitive to the net refractive index of the core, not to the difference between the core and the cladding as for the LPG. The dynamics of the coupling between the modes in LPGs has also been reported [78].

To prevent the fiber from out-gassing prematurely, it should be stored at low temperatures (−70°C) until it is used.

The diffusion time taken to reduce the hydrogen initial concentration, C_0/e, in the core is shown in Fig. 2.12a as a function of fiber diameter, at room temperature (20°C). Also shown is the diffusion time for standard fiber as a function of temperature (Fig. 2.12b).

2.4.5 Rare-earth-doped fibers

For a vast number of applications, such as fiber lasers and amplifiers, it is necessary to fabricate gratings in rare-earth-doped fibers. It is more difficult to write Bragg gratings in these fibers than in standard fibers. Worse, germanium is replaced by aluminum (Al_2O_3) to reduce the effect of quenching and lifetime shortening [79]. The lack of germanium reduces the photosensitivity of optical fibers, even with hydrogen sensitization, although gratings have been reported [46]. Gratings can be formed in most fibers, but the index changes remain weak ($<10^{-4}$) in all cases with 240-nm irradiation except in hydrogen-loaded Al/Ce or Al/Tb. With 193-nm irradiation, Al/Yb/Er fiber has shown index changes of 10^{-4} while hydrogen loading increases this figure to $\sim 10^{-3}$. The conclusion is that hydrogen loading improves the photosensitivity of germanium-free rare-earth-doped fibers. However, only a small subset of Er, Nd, and Ce and Tb-doped silicate fibers show reasonable photosensitivity ($>10^{-4}$) [46].

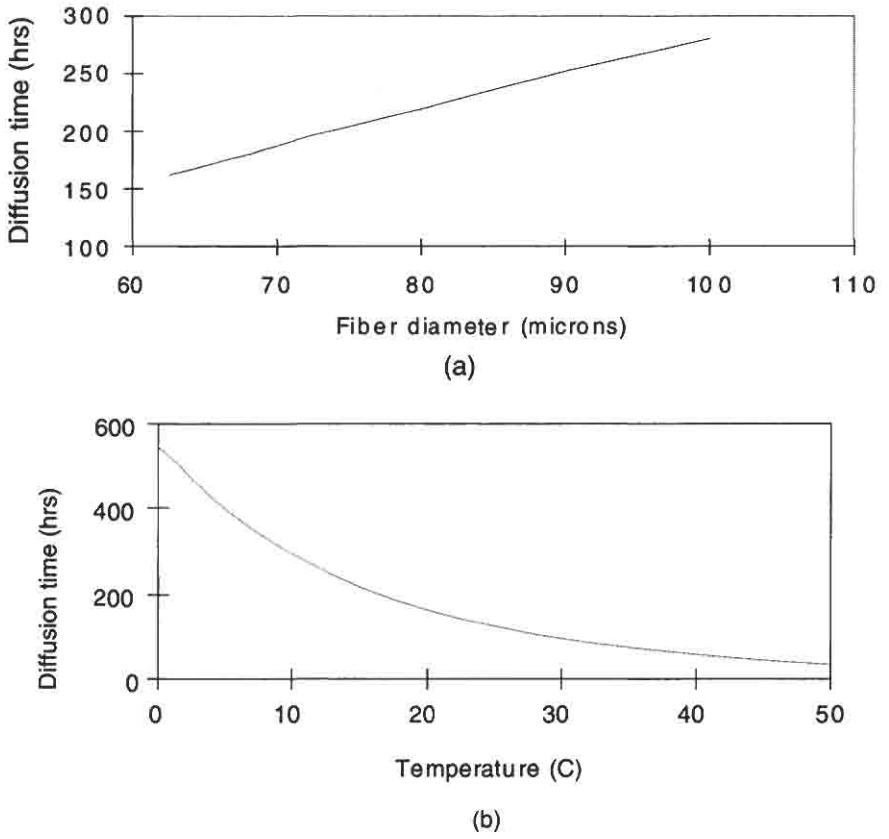

Figure 2.12: Out-diffusion time (1/*e* of initial concentration, C_0 of hydrogen as a function of fiber diameter at 20°C (a), and the diffusion time for a standard fiber as a function of temperature (b) (courtesy F. Bhakti).

The direct writing of gratings in RE fibers is limited to longish lengths, which suits the fabrication of narrow-band DFB fiber lasers. All gratings are of Type I or Type II; Type IIA has not been reported. A summary of the results on the most photosensitive fibers is listed in Table 2.1.

2.5 Densification and stress in fibers

There is increasing evidence that densification and stress increase in optical fibers contributes to the change in the refractive index [84–87]. Surface

TABLE 2.1: League table of rare-earth-doped silica photosensitive fiber.

Core dopant with Al, Ge-free	UV source: pulsed (nm)	$\sim\Delta n$ (pk–pk)	Reference
Undoped reference sample	193	5×10^{-5}	46
Eu^{2+}	248	2.5×10^{-5}	80
Ce^{3+}	265	3.7×10^{-4}	43, 81
Yb^{3+} and Er^{3+}	193	10^{-4}	46
P and Ce^{3+}	266	1.4×10^{-4}	82
Ce^{3+} and H_2	240	1.5×10^{-3}	43
Tb^{3+} and H_2	240	6×10^{-4}	83
Er^{3+} and H_2	235	5×10^{-5}	43
Tm^{3+} and H_2	235	8×10^{-5}	43
Yb^{3+}: Er^{3+} and H_2	193	5×10^{-4}	43

AFM scans of unetched samples show that the surface densifies in the UV illuminated regions [100]. In Fig. 2.13 is shown an atomic force microscope (AFM) scan of the surface of an Andrew Corp. D-fiber. After a grating has been written, the fiber is etched in buffered solution (3 vol% NH_4F 40%, 1 vol of HF 49% diluted with 50% saturated citric acid) with HF 25% for 110 minutes. The revealed pattern is indicative of structural modification in the glass, which influences the etch rate [88]. Stress measurement made optically show that the tensile stress increases in the core, *reducing* the induced refractive index change by as much as 30% [101] (see Chapter 9).

2.6 Summary of photosensitive mechanisms in germanosilicate fibers

There appear to be three routes by which a photo-induced refractive index change occurs in germanosilicate optical fibers:

1. Through the formation of color centers (GeE′)
2. Densification and increase in tension
3. Formation of GeH

Broadly speaking, all three mechanisms prevail in optical fibers. The relative importance of each contribution depends on the type of optical fiber and the photosensitization process used. Most fibers, if not all, show an increase in the population of GeE′ centers (trapped hole with an oxygen

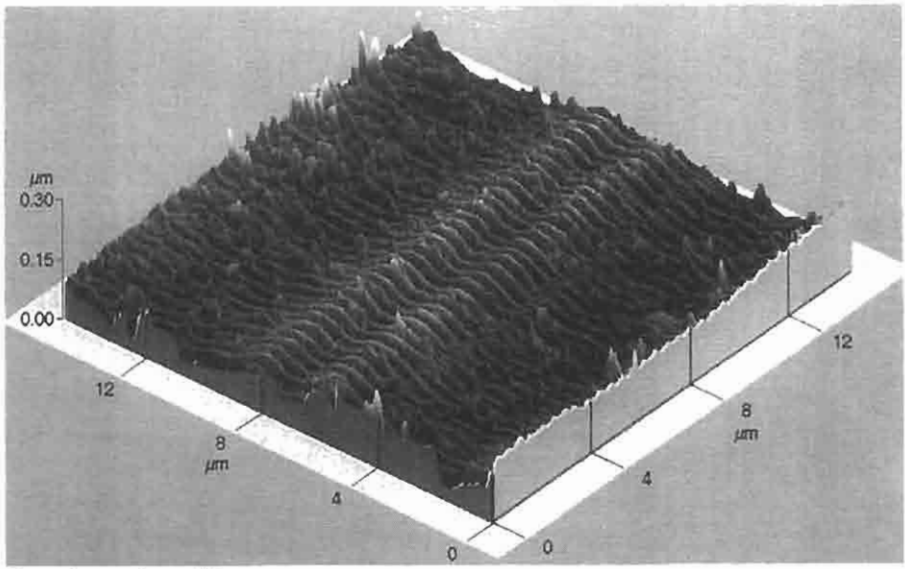

Experimental conditions :

• grating inscription : 8000 pulses at a fluence per pulse of 185 mJ/cm^2, grating pitch = 0.453 µm, R = R_{max}.

•• A.F.M. was performed after etching the fibre for 110 mn using buffered solution BOE mixed with 25% of HF.
BOE is (3 vol. of [NH_4F] 40%, 1 vol. of [HF] 49% diluted by 50% with saturated citric acid).

Figure 2.13: AFM scan of a D-fiber surface. Surface etched after grating inscription to reveal the chemically modified structure (courtesy Marc Douay, Ref. [88]).

vacancy) after UV exposure [89]. This is formed by the conversion of the electron-trapped Ge(I) center, which absorbs at ~5 eV. The change in the population of the GeE′ centers cause changes in the UV absorption spectra, which lead to a change in the refractive index directly through the Kramers–Kronig relationship [90] [Eq. (1.1.4)]. This process is common to all fibers. The color center model, originally proposed by Hand and Russell [91], only explains part of the observed refractive index changes of $\sim 2 \times 10^{-4}$ in nonhydrogenated optical fibers [92,93].

The second mechanism is a structural alteration in the mechanical nature of the glass and was pointed out several years ago by Bernardin and Lawandy [94]. In the model, a collapse of a higher-order ring structure was proposed as a possible effect of irradiation, leading to densification. The densification of silica under UV irradiation is well documented [95].

However, the picture is not as simple, since another mechanism opposes it: the relief of the internal stress frozen in during fiber fabrication, on UV exposure [96,97]. Stress relief can only remove the effect of the frozen-in stress and is therefore strongly dependent on the initial thermoelastic stress at fabrication. There is correlation between fiber drawing tension and the maximum induced index change for Type I gratings but reduced maximum index change for Type IIA [98]. The process of densification has been shown to occur in fibers as evidenced by scans using an atomic force microscope of the surface of D-shaped fibers and in etched fibers [99], and in preform samples that were drawn into a D-shaped fiber [100]. These observations are on the surface of the sample and are unable to replicate the stress profiles within the core of the fiber directly. Direct optical measurement of in-fiber stress has indicated that rather than the relief of the stress, tensile stress actually *increases* with an associated reduction in the average refractive index by ~30% of the observed UV induced refractive index change in non-hydrogen loaded, high-germania-content fibers [101]. The changes in the stress profile of the fiber are consistent with the shift in the Bragg wavelength of a grating during inscription [102].

The third mechanism for the UV induction of the refractive index change is via the formation of Ge–H and the generation of GeE′ centers; it was proposed by Tsai and Friebele [89]. The concentration of the GeE′ have been previously correlated with the presence of the precursor states of the Ge(I) and Ge(II) centers. However, the concentration of GeE′ centers continues to grow despite the saturation of both Ge(I) and Ge(II), indicating that the formation of the E′ centers has another route. The color center model for the changes in the refractive index is supported by the measurements made by Atkins *et al.* [103].

2.7 Summary of routes to photosentization

A method for photosensitizing silica optical fiber is based on the observation that increasing the 240-nm absorption enhances the effect [104]. Thus, reduced germania present as GeO has been shown to have a good photosensitive response. Other defect formers, such as europium [80], cerium [81], and thulium [43], also fall in this category, albeit with a smaller effect. Phosphorus, which is used extensively in the fabrication of germania-doped silica planar waveguides, shows a weak response with

radiation around 240 nm. However, the situation changes with radiation at 193 nm, as has been demonstrated [46].

Silica optical fibers with cores doped with germania, phosphorus, or alumina all exhibit increased photosensitivity when fabricated in a reducing atmosphere of hot hydrogen [105,106]. The negative effect of this type of treatment is the increase in the absorption due to the presence of OH^- ions and also an increase in the refractive index of the core. Flame-brushing, i.e., heating optical fiber or planar silica waveguides using a flame in a hydrogen-rich atmosphere, has also been used for photosensitization [107]. Hydrogen is able to diffuse into the fiber rapidly at elevated temperatures.

Germanosilicate optical fiber codoped with boron has been shown to be highly photosensitive [40]. Another advantage of the presence of boron is the large reduction in the background refractive index, allowing more germania to be added in the core for a given core–cladding index difference. It is believed that with boron physiochemical changes are responsible for the UV-induced index changes (approximately a few thousandths). Boron-codoped fiber gratings decay with temperature more rapidly than pure-germania doped fibers, although there are way to enhance their stability by using burn-in (see Chapter 9). The presence of boron also increases the absorption loss in the 1500-nm window by $\sim 0.1\ \mathrm{dB\ m^{-1}}$. An alternative scheme to circumvent the problems associated with boron is to use Sn codoping with germania [63]. This combination is more difficult to fabricate, but has virtually no additional absorption in the 1500-nm window, has a similar photosensitivity to the B–Ge system, and exhibits better temperature stability. There is no reduction in the refractive index with Sn doping.

Finally, the system that has demonstrated the largest photosensitive response in germanosilicate optical fibers is high-pressure cold hydrogen soaking [66]. It has been demonstrated that nearly every germanium ion is a potential candidate for conversion from the Ge–O to the Ge–H state [108], causing index changes as large as 0.01, although the ultimate magnitude of the index change is not known. Once hydrogenated, these fibers need to be stored at low temperatures to maintain their photosensitivity, since molecular hydrogen diffuses out just as readily as it can be introduced. A major disadvantage of writing gratings into cold-hydrogen-sensitized fiber gratings is the high loss of several decibels per meter at 1320 nm (OH^- absorption). Deuteration eliminates the absorption at 1320 nm, while maintaining the photosensitivity [68]. A summary of the all currently known techniques of photosensitizing fibers is listed in Table 2.2.

TABLE 2.2: Routes to photosensitization of optical fibers.

Fiber type	Fabrication process	Photosensitivity	Advantages	Disadvantages
Standard telecommunications germania-doped fiber ~3 mol%	Standard CVD/ PECVD	Very low: Photosensitive index change, $\delta n \sim 1 \times 10^{-6}$ (except one report of 1×10^{-3} [109])	Easy production, useful for low reflectivity gratings	Very low photosensitivity, low birefringence, good quality fiber
High germania 10–30 mol%	Standard CVD/ PECVD	Low photosensitive index change, slow growth of gratings, $\delta n \sim 1 \times 10^{-4}$	Good quality fiber, easy production	Birefringent, photosensitivity not enough to be useful in untreated fiber
Reduced germania (~10 mol%)	Production depleted oxygen atmosphere	Good photosensitivity, faster growth in index change, $\delta n \sim 5 \times 10^{-4}$	Low OH^- loss, circular cored fiber	Needs high germania (~10 mol%)
Boron–germania codoped	Needs additional calibration since boron reduces core index	Very good, faster increase in index, $\delta n \sim 8 \times 10^{-4}$	Low OH^- loss, can be compatible with standard telecommunication fiber	Difficult preform fabrication, highly stressed, increase in boron induced loss, elliptical core
Hot hydrogenated germania-doped fiber	Preform cooked at 750°C in hydrogen atmosphere	Good photosensitivity, $\delta n \sim$ 8c-4	Needs higher germania than standard tele-communications fiber; easy to store.	Slight increase in OH^- loss

Hot hydrogenated B–Ge codoped fiber	Same as above	Very good, $\delta n \sim 1 \times 10^{-3}$	Can be made compatible with standard telecommunication fiber	High stress, difficult to fabricate as B–Ge fiber. Loss at 1500 nm
High pressure cold hydrogen soaked germania-doped fiber	Easy fabrication since all types of above fiber may be used, including standard telecommunication fiber. But requires high pressure (up to 800Bar) facility	Excellent photosensitivity, $\delta n \sim 1 \times 10^{-2}$ in standard telecommunications fiber	Extremely versatile	OH loss with increase in index change. The loss can be ~0.1 dB per grating. Limited shelf life unless stored at low temperatures to prevent out-diffusion of H_2
High pressure cold deuterium soaked germania-doped fiber	Same as above	Same as above	No increase in loss at 1300/1500 nm since OD(OH) overtones are not in second or third telecommunications window	Extremely expensive option. Also limited shelf life unless stored at low temperatures to prevent out-diffusion of D_2
High-pressure hydrogen soaking of phosphorus rare-earth-doped fiber (Ge free)	Same as above	Can photosensitize many types of doped silica fibers	Intracore cavity fiber gratings possible for fiber lasers—no splice loss.	Requires 193-nm radiation for useful index changes and ease of writing

2.7.1 Summary of optically induced effects

The chemical reactions that take place in photosensitive optical fiber exposed to UV radiation are probably never going to be understood completely. However, several known factors influence the index change.

1. Bleaching of the 240-nm GeO band in reduced germania fibers. This has been measured and alludes to the following picture of chemical modification. The Ge–Si bonds break, liberating an electron, which may be retrapped at another defect site. What remains is the type of picture seen in Fig. 2.2 (GeE′). It is not known whether a volumetric change occurs as well. It is likely that, owing to the confinement of the photosensitive species within a massive cladding, any physical relaxation or contraction of molecular bonds will result in a stressed state. Recently, the stress change in fiber cores has been theoretically modeled and also measured using optical methods [110], with good agreement between the two. Douay *et al.* [99] have etched fibers and preforms previously exposed to interfering UV beams and found that a relief grating is revealed. Although this is not direct evidence that physical changes occur on UV exposure, it does show that the chemistry has indeed been altered. Riant *et al.* [100] performed atomic force microscopy (AFM) on the surface of D-shaped fibers in which gratings have been written. The surface of the fiber, a few microns above the photosensitive core of germanin-doped silica, showed a surface relief directly indicating stress changes. Therefore, not only does the absorption in the UV change, but so does the density of oscillators with UV exposure, both of which alter the refractive index based on the Kramers–Kronig rules. However, it must be remembered that the molecules within the core are not free to change their shape, but are elastically coupled to the mass in the cladding via bonds that remain predominantly unchanged. This is the basis for the induced stress and for part of the index modification by the stress-optic coefficient. Russell *et al.* [111] have estimated that a strain of only 10^{-4} is necessary to induce an index change in the effective index of the mode by the *same* order of magnitude. It is well known that fiber drawing conditions and stress annealing can alter the refractive index of boron-doped glasses [112].

2. There is a change in the position of the band edge of germania-doped silica in the deep-UV spectrum, which alters the refractive index after UV exposure. This effect is difficult to quantify owing to the problems associated with measurements in the vacuum ultraviolet and the low transparency of silica below a wavelength of ~190 nm, although some measurements have been made [113], suggesting that there is no shift in the edge, just an increase in the absorption in the deep UV.
3. High-temperature hydrogen treatment reduces germania, producing an enhanced concentration of GeO molecules [114]. Again bleaching of the absorption at 240 nm partly contributes to the index change. Other effects as in points 1 and 2 above prevail. Chemically, the reduction process may occurs as follows:

4. Molecular hydrogen. The suggested reaction is the formation of GeH and OH ions from a Ge(2) defect. The GeH is responsible for the change in the refractive index via the Kramers–Kronig rule. The possible route may be as follows:

It is not clear what the reactions with a pure alumina doped silica core may be, but it is possible that a similar set of observations may occur; the addition of phosphorus in germania-doped fibers reduces the concentration of GeE' centers, increasing with increased fabrication temperatures or reducing conditions [115].

Figure 2.14 compares a set of different fibers exposed to the same intensity of radiation at 262 nm for different times. The comparison shows the refractive index growth rate for fiber with different photosensitization treatments when exposed to UV radiation, per mol% Ge in the fiber,

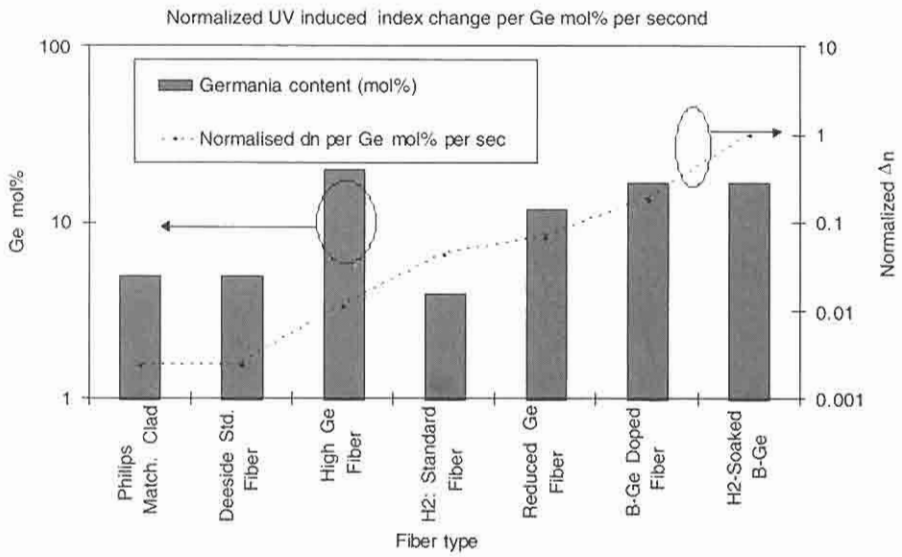

Figure 2.14: Comparison of time-averaged growth rate of the UV-induced refractive index change for different fibers compared to cold H_2-soaked:B-Ge fiber on the right column. Maximum index change recorded for the H–BGe codoped fiber was 6.76×10^{-3}. The UV source was a quadrupled diode pumped QS Nd:YLF laser operating at 262 nm with 60-mW writing power and used with a phase mask. This is a direct comparison of the induced index change in Type I gratings showing the sensitivity to UV radiation (adapted from Ref. [40]).

normalized to the fastest fiber: the H_2: BGe, which writes an 87% reflective, 1.5-mm long grating in 10 seconds.

References

1 Kleinmann D. A., "Nonlinear dielectric polarization in optical media," *Phys. Rev.* **126**(6), 1977–1979 (1962).

2 Kazansky P. G., Russell P. St. J., and Takebe H.,"Glass fiber poling and applications," *Lightwave Technol.* **15**(8), 1484–1493 (1997).

3 Griscom D. L., "Optical properties and structure of defects and structure of defects in silica glass," *Ceramic Soc. Jap.* **99**(10), 923–942 (1991).

4 Neustruev V. B., "Colour centres in germanosilicate glass and optical fibers," *J. Phys. Condens. Matter* **6**, 6901–6936 (1994).

5 Glass A. M., "The photorefractive effect," *Opt. Engg.* **17**, 470–479 (1978).

6 Fleming S. C., Fujiwara T., and Wong D., "UV excited poling of germanosilicate fibre," in *Photosensitivity and Quadratic Nonlinearity in Glass Waveguides: Fundamentals and Applications,* Vol. 22, 1995 OSA Technical Series (Optical Society of America, Washington DC, 1995), paper SUD1, pp. 180–183 (1995).

7 Myers R. A., Mukherjee N., and Brueck S. R. J., "Large second order nonlinearity in poled fused silica," *Opt. Lett.* **16**, 1732–1734 (1991).

8 Mukerjee N., Myers R. A., and Brueck S. R. J., "Dynamics of second order nonlinearities in poled silicate fibers," *J. Opt. Soc. Am. B* **11**, 665–669 (1994).

9 Dianov E. M., Kazansky P. G., Prokohorov A. M., and Stephanov D. Yu, "Photoinduced second-harmonic generation in glasses and glass optical fibers: Recent experiments," *Mol. Cryst. Liq. Cryst. Sci. Technol. Sec. B, Nonlinear Optics* **3**, 329–340 (1992).

10 Nagel S., MacChesney J. B., and Walker K. L., "An overview of the modified chemical vapor deposition (MCVD) process and performance," *IEEE J. Quantum Electron.* **QE-18**(4) 459–476, (1982).

11 Hibino Y. and Hanafusa H., "Defect structure and formation mechanism of drawing induced absorption at 630 nm in silica optical fibers," *J. Appl. Phys.* **60**, 1797 (1986).

12 Hibino Y. and Hanafusu H., "ESR study on E' centres induced by optical drawing process," *Jap. Journ. Appl. Phys.* **22**(12), 766–768 (1983).

13 Kaiser P., "Drawing induced coloration in vitreous silica fibers," *J. Opt. Soc. Am.* **64**, 475 (1974).

14 Lawandy N. M., "Light induced transport and delocalization in transparent and amorphous systems," *Opt. Commun.* **74**, 180–184 (1989).

15 Stapelbroek M., Griscom D. L., Friebele E. J., and Siegel G. H., "Oxygen-associated trapped-hole centers in high purity fused silica," *J. Non-Cryst. Solids* **32**, 313 (1979).

16 Nishikawa H., Tohmon R., Okhi Y., Hama Y., and Nagasawa K., "325nm absorption band by peroxy linkage in pure silica core fibre," in *Tech. Digest of Conf. on Optical Fiber Commun.,* OFC'89, p. 158 (1989).

17 Fribele E. J., Griscom D. L., and Siegel, G. H., Jr., "Defect centers in germania doped silica core optical fiber," *J. Appl. Phys.* **45**, 3424–3428 (1974).

18 Kawazoe H., "Effects of modes of glass formation on the structure of intrinsic or photoinduced defects centered on III, IV, or V cations in oxide glasses," *J. Non-Cryst. Solids* **71**, 213–234 (1985).

19 Tsai T. E., Griscom D. L., Fribele E. J., and Fleming J. W., "Radiation induced defect centers in high purity GeO_2 glass," *J. Appl. Phys.* **62**, 2262–2268 (1987).

20 Tsai T. E., Griscom D. L., and Fribele E. J., "On the structure of Ge-associated defect centers defect in irradiated high purity GeO_2 and Ge-doped SiO_2 glass," *Diffusion and Defect Data* **53–54**, 469–476 (1987).

21 Honso H., Abe Y., Kinser D. L., Weeks R. A., Muta K., and Kawazoe H., "Nature and origin of the 5 eV band in SiO_2:GeO_2 glasses," *Phys. Rev. B* **46**, II-445–II-451 (1995).

22 Hughes R. C., "Charge carrier transport phenomenon in amorphous SiO_2, direct measurement of the drift and mobility and lifetime," *Phys. Rev. Lett.* **30**, 1333–1336 (1973).

23 Isoya J., Weil J. A., and Claridge R. F. C., "The dynamical interchange and relationship between germanium centers in a-quartz," *J. Chem. Phys.* **62**, 4876–4884 (1978).

24 Malo B., Albert J., Bilodeau F., Kitagawa T., Johnson D. C., Hill K. O., Hattori K., Hibino Y., and Gujrathi S., "Photosensitivity in phosphorus doped silica glass and optical waveguides," *Appl. Phys. Lett.* **65**, 394–396 (1994).

25 Griscom D. L. and Mizuguchi M., "Determination of the visible range optical absorption spectrum of peroxy radicals in gamma irradiated fused silica," in *Bragg Gratings, Photosensitivity and Poling in Glass Fibers and Waveguides: Fundamentals and Applications*, Vol. 17, 1997 OSA Technical Series (Optical Society of America, Washington DC, 1997), paper JMD2, pp. 139–141 (1997).

26 MacDonald R. L. and Lawandy N. M., "Efficient second harmonic generation into the UV using optically encoded silicate glasses. *Opt. Lett.*, **18**(8), 595–597 (1993).

27 Dominic V. and Feinberg J., "Spatial shape of the dc-electric field produced by intense light in glass," *Opt. Lett.* **18**, 784–786 (1993).

28 Kashyap R., Maxwell G. D., and Williams D. L., "Photoconduction in Ge-P doped silica waveguides," *Appl. Phys. Lett.* **62**(3), 214–216 (1993).

29 Bagratshivilii V., Tsypina S. I., Chernov P. V., Rybaltovskii A. A. O., Zavorotny Y. S., Alimpiev S. S., Simanovskii Y. O., Dong L., and Russell P. St., "UV laser induced photocurrent in oxygen deficient silica and germanosilicate glasses," in *Photosensitivity and Quadratic Nonlinearity in Glass Waveguides: Fundamentals and Applications*, Vol. 22, 1995 OSA Technical Series (Optical Society of America, Washington DC, 1995), paper SUA1, pp. 66–69 (1995).

30 Purcell T. and Weeks R. A., "Electron spin resonance and optical absorption in GeO_2," *J Chem. Phys.* **78**, 1638–1651, (1987).

31 Archambault J-L., Reekie L., and Russell P. St. J., "100% reflectivity Bragg reflectors produced in optical fibres by single excimer pulses," *Electron. Lett.* **29**(5), 453 (1993).

32 Xie W. X., Douay M., Bernage P., Niay P., Bayon J. F., and Georges T., "Second order diffraction efficiency of Bragg gratings written within germanosilicate fibres," *Opt. Commun.* **101**, 85 (1993).

33 Williams D. L., Davey S. T., Kashyap R, Armitage J. R., and Ainslie B. J., *SPIE* **1513** 158, *Glasses for Optoelectronics* II, ECO4, The Hague (1991).

34 Poumellec B., Niay P., Douay M., and Bayon J. F., "The UV induced refractive index grating in Ge:SiO_2 preforms: additional CW experiments and the macroscopic origin of the index change in index," *J. Phys. D, Appl. Phys.* **29**, 1842–1856 (1996).

35 Cohen A. J. and Smith H. L., "Ultraviolet and infrared absorption of fused germania," *J. Phys. Chem.* **7**, 301–306 (1958).

36 Dong L., Pinkstone J., Russell P. St. J., and Payne D. N., "Study of UV absorption in germanosilicate fiber performs," in *Tech. Digest of Conf. on Lasers and Opto-Electronics, CLEO'94,* pp. 243–245 (1994).

37 Kohketsu M., Awazu K., Kawazoe H., and Yamane M., "Photoluminescence in VAD SiO_2:GeO_2 glasses sintered under reducing or oxidizing conditions," *Jap. J. Appl. Phys.* **28**(4), 622–631, 1989.

38 Skuja L. N., Truhkin A. N., and Plaudis A. E., "Luminescence in germanium doped glassy SiO_2," *Phys. Stat. Sol. A* **84**, K153–157 (1984).

39 Dong L., Pinkstone J., Russell P. St. J., and Payne D. N., "Ultraviolet absorption in modified chemical vapour deposition performs," *J. Opt. Soc. Am. B.* **11**, 2106–2111 (1994).

40 Williams D. L., Ainslie B. J., Kashyap R., Maxwell G. D., Armitage J. R., Campbell R. J., and Wyatt R., "Photosensitive index changes in germania doped silica fibers and waveguides," in *Photosensitivity and Self Organization in Optical Fibers and Waveguides, SPIE 2044,* pp. 55–68 (1993).

41 Albert J., Malo B., Hill K. O., Bilodeau F., Johnson D. C., and Theriault S., "Comparison of one-photon and two photon effects in photosensitivity of germanium doped silica optical fibers exposed to intense ArF excimer laser pulses," *Appl. Phys. Lett.* **67**, 3519–3521 (1995).

42 Niay P., Bernage P., Douay M., Taunay T., Xie W. X., Martinelli G., Bayon J. F., Poignant H., and Delevaque E., "Bragg grating photoinscription within various types of fibers and glasses," in *Photosensitivity and Quadratic Nonlinearity in Glass Waveguides: Fundamentals and Applications,* Vol. 22, 1995 OSA Technical Series (Optical Society of America, Washington DC, 1995), paper SUA1, pp. 66–69 (1995).

43 Tanuay T., Niay P., Bernage P., Douay M., Xie W. X., Puerer D., Cordier P., Bayon J. F., Poignant H., Delevaque E., and Poumellec B., "Bragg gratings

inscription within strained monomode high NA germania doped fibers: Part I—Experimentation," *J. Phys D: Appl. Phys.* **30**(1), 40–52, (1996).

44 Riant I. and Sansonetti P., "Influence of fiber drawing tension on photosensitivity in hydrogenated and unhydrogenated fibers," in *Tech. Digest of Conf. On Opt. Fiber Commun., OFC'98,* pp. 1–2 (1998).

45 Fribele E. J., Siegel G. H., and Griscom D. L., "Drawing induced defect centers in fused silica core fiber," *Appl. Phys. Lett.* **28**, 516–518 (1976).

46 Douay M., Xie W. X., Taunay T., Bernage P., Niay P., Cordier P., Poumellec B., Dong L., Bayon J. F., Poignant H., and Delevaque E., "Densification involved in the UV based photosensitivity of silica glasses and optical fibers," *J. Lightwave Technol.* **15**(8), 1329–1342 (1997).

47 Xie W. X., Niay P., Bernage P., Douay M., Bayon J. F., Georges T., Monerie M., and Poumellec B., "Experimental evidence of two types of photorefractive effects occurring during photoinscription of Bragg gratings within germanosilicate fibers," *Opt. Commun.* **104**, 185–195 (1993).

48 Grüner-Nielsen L. and Hübner J., Photosensitive fiber for highly reflective Bragg gratings," in *Tech. Digest of Conf. on Opt. Fiber Commun., OFC'97,* paper WL16, p. 178, (1997).

49 Williams D. L., Ainslie B. J., Armitage J. R., Kashyap R., and Campbell R. J., "Enhanced photosensitivity in germanium doped silica fibers for future optical networks," in *Proc. of the 18th European Conf. on Optical Commun., ECOC'92,* paper We B9-5, 425–428 (1992).

50 See, for example, Lemaire P. J., "Reliability of optical fibers exposed to hydrogen: prediction of long-term loss increases," *Opt. Eng.* **30**(6), 780–789 (1991).

51 Pavy D., Mosian M., Saada S., Cholet P., Leprince P., and Marrec J., in *Proc. ECOC'86,* pp. 132–141 (1986).

52 Dianov E. M., Golant K. M., Mashinsky V. M., Mededkov O. I., Nikolin I. V., Sazhin O. D., and Vasiliev S. A., "Highly photosensitive germanosilicate fiber codoped with nitrogen," in *Bragg Gratings, Photosensitivity and Poling in Glass Fibers and Waveguides: Fundamentals and Applications,* Vol. 17, 1997 OSA Technical Series (Optical Society of America, Washington DC, 1997), paper BME2, pp. 153–155 (1997).

53 Camlibel I, Pinnow D. A., and Dabby F. W., "Optical aging characteristics of borosilicate clad fused silica core fiber waveguides," *Appl. Phys. Lett.* **26**(4), 185–187 (1975).

54 Williams D. L., Ainslie B. J., Armitage J. R., Kashyap R., and Campbell R. J., "Enhanced UV photosensitivity in boron codoped germanosilicate optical fibres," *Electron. Lett.* **29**, 45–47 (1993).

55 Kashyap R., Williams D. L., and Smith R. P., "Novel liquid and liquid crystal cored fibre Bragg gratings," in *Bragg Gratings, Photosensitivity and Poling in Glass Fibers and Waveguides: Fundamentals and Applications,* Vol. 17, 1997 OSA Technical Series (Optical Society of America, Washington DC, 1997), paper BSuB5, pp. 25–27 (1997).

56 Dong L., Loh W. H., Caplen J. E., Hsu K., and Minelly J. D., "Photosensitive Er/Yb optical fibers for efficient single frequency fiber lasers," in *Tech. Digest. of Conf. on Opt. Fiber Commun., OFC'97,* pp. 29–30 (1997).

57 Kashyap R., Holmes M. H., Williams D. L., and Smith R. P., "Ultra-narrow band radiation mode filters," IOP, London, 1 May 1997.

58 Holmes M. J., Kashyap R., Wyatt R., and Smith R. P., "Development of radiation mode filters for WDM," *IEE Colloquia on multi-wavelength Networks: Devices Systems and Network Implementations, Ref. 1998/296,* June 1998.

59 Bonino S., Norgia M., Riccardi E., and Schiano M., "Measurement of polarisation properties of chirped fibre gratings," in *Technical Digest of OFMC'97,* pp. 10–13, (1997).

60 Kashyap R., Unpublished. Type IIA gratings have been regularly observed in B–Ge fibers with (15 mol% Ge) during writing with a CW 244-nm laser between 20 and 40 minutes of exposure. Presently, there is no other public domain data on this.

61 Douay M., private communication.

62 Baker S. R., Rourke H. N., Baker V., and Goodchild D., "Thermal decay of fiber Bragg gratings written in borongermania codoped silica fiber," *J. Lightwave Technol.* **15**(8), 1470–1477 (1997).

63 Dong L., Cruz J. L., Reekie L., Xu M. G., and Payne D. N., "Large photoinduced changes in Sn-codoped germanosilicate fibers," in *Photosensitivity and Quadratic Nonlinearity in Glass Waveguides: Fundamentals and Applications,* Vol. 22, 1995 OSA Technical Series (Optical Society of America, Washington DC, 1995), paper SUA2, pp. 70–73 (1995).

64 See, for example, Lemaire P. J., Watson H. A., DiGiovanni D. J., and Walker K. L., "Prediction of long term hydrogen induced loss increases in Er-doped amplifiers," *IEEE. Photonic Technol. Lett.* **5**(2), 214–217 (1993), and references therein.

65 Lemaire P. J., "Reliability of optical fibers exposed to hydrogen: prediction of long-term loss increases," *Opt. Eng.* **30**(6), 780–789 (1991).

66 Lemaire P., Atkins R. M., Mizrahi V., and Reed W. A., "High pressure H_2 loading as a technique for achieving ultrahigh UV photosensitivity and thermal sensitivity in GeO_2 doped optical fibres," *Electron. Lett.* **29**(13), 1191 (1993).

67 Atkins R. M., Lemaire P. J., Erdogan T., and Mizrahi V., "Mechanisms of enhanced UV photosensitivity via hydrogen loading in germanosilicate glasses," *Electron. Lett.* **29**, 1234–1235 (1993).

68 Lemaire P. J., Vengsarkar A. M., Reed W. A., and Mizrahi V., "Refractive index changes in optical fibers sensitized with molecular hydrogen," in *Technical Digest of Conf. on Opt. Fiber Commun., OFC'94,* pp. 47–48, (1994).

69 Martin J., Atkins G., Ouellette F., Tetu M., Deslauriers J., and Dugay M., "Direct correlation between luminescence and refractive index change in photosensitive Ge-doped and hydrogenated optical fibre," in *Photosensitivity and Quadratic Nonlinearity in Glass Waveguides: Fundamentals and Applications,* Vol. 22, 1995 OSA Technical Series (Optical Society of America, Washington DC, 1995), paper PMA2, pp. 200–203 (1995).

70 Kashyap R., unpublished (1997).

71 Atkins R. M. and Lemaire P. J., "Effects of elevated temperature on hydrogen exposure on short wavelength optical loss and defect concentration in germanosilicate optical fibers," *J. Appl. Phys.* **72**(2), 344–348 (1992).

72 Carslaw H. S. and Jaeger J. C., *Conduction of Heat in Solids,* Clarendon Press, Oxford (1978).

73 Bhakti F., Larrey J., Sansonetti P., and Poumellec B., "Impact of in-fiber and out-fiber diffusion on central wavelength of UV-written long period gratings," in *Bragg Gratings, Photosensitivity and Poling in Glass Fibers and Waveguides: Fundamentals and Applications,* Vol. 17, 1997 OSA Technical Series (Optical Society of America, Washington DC, 1997), paper BSuD2, pp. 55–57 (1997).

74 Stone J., "Interactions of hydrogen and deuterium with silica optical fibers: a review," *J. Lightwave Technol.* **5**(5), 712–733 (1987).

75 Shackelford J. F., Studt P. L., and Fulrath R. M., "Solubility of gases in glass: II: He, Ne, H_2 in fused silica," *J Appl. Phys.* **43**(4), 1619–1629 (1972).

76 Malo B., Albert J., Kill K. O., Bilodeau F., and Johnson D. C., "Effective index drift from molecular hydrogen loaded optical fibres and its effect on Bragg grating fabrication," *Electron. Lett.* **30**(5), 442–444 (1994).

77 Miller T. M., "Atomic and molecular polarizabilities," in *CRC Handbook of Chemistry and Physics,* pp. E68–E72, CRC Press, Boca Raton, FL (1989).

78 Jang J. N. and Kwack K. H., "Dynamics of coupling by H_2 diffusion in long period grating filters," in *Bragg gratings, Photosensitivity and Poling in Glass Fibers and Waveguides: Fundamentals and Applications,* Vol. 17, 1997 OSA Technical Series (Optical Society of America, Washington DC, 1997), paper BMG10, pp. 213–215 (1997).

79 Desurvire E., in *Erbium-Doped Fiber Amplifiers: Principles and Applications*. Wiley, New York (1994).

80 Hill K. O., Malo B., Bilodeau F., Johnson D. C., Morse T. F., Kilian A., Reinhart L., and Kyunghwan Oh., "Photosensitivity in Eu^{2+}:Al_2O_3-doped-core fibre: preliminary results and application to mode converters," *Proc. Conference on Optical Fiber Communications, OFC'91, paper PD3-1,* pp. 14–17 (1991).

81 Broer M. M., Cone R. L., and Simpson J. R., "Ultraviolet-induced distributed-feedback gratings in Ce^{3+} doped silica optical fibres," *Opt. Lett.* **16**(18), 1391–1393 (1991).

82 Dong L., Wells P. J., Hand D. P., and Payne D. N.,"Photosensitivity in Ce^{3+} doped optical fibers," *J. Opt. Soc. Am. B* **10**, 89–93 (1993).

83 Taunay T., Bernage P., Martenelli G., Douay M., Niay P., Bayon J. F., and Poignant H., "Photosensitization of terbium doped aluminosilicate fibers through high pressure H_2 loading," *Opt. Commun.* **133**, 454–462 (1997).

84 Douay M., Ramecourt D., Taunay T., Niay P., Bernage P., Dacosta A., Mathieu C., Bayon J. F., and Poumellec B., "Microscopic investigations of Bragg grating photowritten in germanosilicate fibers," in *Photosensitivity and Quadratic Nonlinearity in Glass Waveguides: Fundamentals and Applications,* Vol. 22, 1995 OSA Technical Series (Optical Society of America, Washington DC, 1995), paper SAD2, pp. 48–51.

85 Riant I., Borne S., Sansonetti P., and Poumellec B., "Evidence of densification in UV-written Bragg gratings in fibers," in *Photosensitivity and Quadratic Nonlinearity in Waveguides: Fundamentals and Applications,* Vol. 22, 1995, OSA Technical Digest Series (Optical Society of America, Washington DC, 1995), pp. 51–55.

86 Douay M., Xie W. X., Taunay T., Bernage P., Niay P., Cordier P., Poumellec B., Dong L., Bayon J. F., Poignant H., and Delevaque E., "Densification involved in the UV based photosensitivity of silica glasses and optical fibers," *J. Lightwave Technol.* **15**(8), 1329–1342, (1997).

87 Fonjallaz P. Y., Limberger H. G., Salathé R. P., Cochet F., and Leuenberger B., "Tension increase correlated to refractive index change in fibers containing UV written Bragg gratings," *Opt. Lett.* **20**(11), 1346–1348 (1995).

88 Courtesy Marc Douay, Bertrand Poumellec and Pierre Sansonetti. The AFM scan was performed after a grating with a 0.453-μm pitch had been inscribed with 8000 pulses at 185 mJ/cm^2 at 244 nm, doubled dye pumped by a XeCl laser, before etching. Details may be found in Ref. [86].

89 Tsai T. E., Williams G. M., and Friebele E. J., "Index structure of fiber Bragg gratings in Ge-SiO_2 fibers," *Opt. Lett.* **22**(4), 224–226 (1997).

90 Tsai T. E. and Friebele E. J., "Kinetics of defect centers formation in Ge–SiO_2 fibers of various compositions," in *Bragg Gratings, Photosensitivity and Poling in Glass Fibers and Waveguides: Applications and Fundamentals,* Vol. 17, 1997 OSA Technical Digest Series (Optical Society of America, Washington DC, 1997), pp. 101–103.

91 Hand D. P. and Russell P. St. J., "Photoinduced refractive index changes in germanosilicate optical fibers," *Opt. Lett.* **15**(2), 102–104 (1990).

92 Williams D. L., Davey S. T., Kashyap R., Armitage J. R., and Ainslie B. J., "Direct observation of UV induced bleaching of 240 nm absorption band in photosensitive germanosilicate glass fibres," *Electron. Lett.* **28**(4), 369 (1992).

93 Dong L., Archambault J. L., Russell P. St. J., and Payne D. N., *Proc. ECOC'94,* 997 (1994).

94 Bernardin J. P. and Lawandy N. M., "Dynamics of the formation of Bragg gratings in germanosilicate optical fibers," *Opt. Commun.* **79**, 194 (1990).

95 Rothschild M., Erlich D. J., and Shaver D. C., "Effects of excimer irradiation on the transmission, index of refraction, and density of ultraviolet grade fused silica," *Appl. Phys. Lett.* **55**(13), 1276 (1989).

96 Sceats M. G. and Krug P. A., "Photoviscous annealing—dynamics and stability of photorefractivity in optical fibers," *SPIE 2044,* 113–120 (1993).

97 Wong D., Poole S. B., and Skeats M. G., "Stress birefringence reduction in elliptical-core fibers under ultraviolet irradiation," *Opt. Lett.* **24**(17), 1773 (1992).

98 Riant I. and Poumellec B., "Influence of fiber drawing tension on photosensitivity in hydrogenated and nonhydrogenated fibers," in *Tech. Digest of Conf. on Opt. Fib. Commun, OFC'98,* paper TuA1, pp. 1–2 (1998).

99 Douay M., Ramecourt D., Tanuay T., Bernage P., Niay P., Dacosta D., Mathiue C., Bayon J. F., and Poumellec B., "Microscopic investigations of Bragg gratings photowritten in germanosilicate fibers," in *Photosensitivity and Quadratic Nonlinearity in Waveguides: Fundamentals and Applications,* Vol. 22, 1995 OSA Technical Digest Series (Optical Society of America, Washington, DC, 1995), pp. 48–51.

100 Riant I., Borne S., Sansonetti P., and Poumellec B., "Evidence of densification in UV-written Bragg gratings in fibers," in *Photosensitivity and Quadratic Nonlinearity in Waveguides: Fundamentals and Applications,* Vol. 22, 1995 OSA Technical Digest Series (Optical Society of America, Washington, DC, 1995), pp. 51–55.

101 Limberger H. G., Fonjallaz P. Y., and Salathé R. P., "UV induced stress changes in optical fibers," in *Photosensitivity and Quadratic Nonlinearity in*

Waveguides: Fundamentals and Applications, Vol. 22, 1995 OSA Technical Digest Series (Optical Society of America, Washington, DC, 1995), pp. 56–60.

102 Douay M., Xie W. X., Taunay T., Bernage P., Niay P., Cordier P., Poumellec B., Dong L., Bayon J. F., Poignant H., and Delevaque E., "Densification involved in the UV based photosensitivity of silica glasses and optical fibers," *J Lightwave Technol.* **15**(8), 1329–1342 (1997).

103 Atkins R. M., Mizrahi V., and Erdogan T., "248 nm induced vacuum UV spectral changes in optical fibre preform cores: support for a colour centre model of photosensitivity," *Electron. Lett.* **29**(4), 385 (1993).

104 Williams D. L., Anslie B. J., Kashyap R., Maxwell G. D., Armitage J. R., Campbell R. J., and Wyatt R., "Photosensitive index changes in germania doped silica glass fibers and waveguides" *SPIE* **2044**, 55–68, (1993).

105 Maxwell G. D., Kashyap R., Ainslie B. J., Williams D. L., and Armitage J. R., "UV written 1550 nm reflection filters in singlemode planar silica waveguides," *Electron. Lett.* **28**(22), 2106–2107, (1992).

106 Meltz G. and Morey W. W., "Bragg grating formation and germanosilicate fiber photosensitivity," *SPIE* **1516**, 185–199 (1991).

107 Bilodeau F., Malo B., Albert J., Johnson D. C., Hill K. O., Hibino Y., Abe M., and Kawachi M., "Photosensitization in optical fiber and silica on silicon/silica waveguides," *Opt. Lett.* **18**, 953–955 (1993).

108 Krol D. M., Atkins R. M., and Lemaire P. J., "Photoinduced second-harmonic generation and luminescence of defects in Ge-doped silica fibers," *SPIE* **1516**, 38–46 (1991).

109 Limberger H. G., Fonjallaz P. Y., and Salathé R., "Spectral characterization of photoinduced high efficient Bragg gratings in standard telecommunication fibers," *Electron. Lett.* **29**(1), 47–49 (1993).

110 Fonjallaz P. Y., Limberger H. G., Salathé R., Cochet F., and Leuenberger B., "Tension increase correlated to refractive index change in fibers containing UV written Bragg gratings," *Opt. Lett.* **20**(11), 1346–1348 (1995).

111 Russell P. St. J., Hand D. P., Chow Y. T., and Poyntz-Wright L. J., "Optically-induced creation, transformation and organisation of defects and colour centres in optical fibres," *SPIE* **1516**, 47–54 (1991).

112 Camlibel I., Pinnow D. A., and Dabby F. W., "Optical ageing characteristics of borosilicate clad fused silicacore fibre optical waveguides," *Appl. Phys. Lett.* **26**(4), 185–187 (1975).

113 Atkins R. M., Mizrahi V., and Erdogan T., "248 nm induced vacuum UV spectral changes in optical fibre preform cores: Support for the colour centre model of photosensitivity," *Electron. Lett.* **29**(4), 385 (1993).

114 Iino A., Kuwabara M., and Kokura K., "Mechanisms of hydrogen induced losses in silica based optical fibers," *J. Lightwave Technol.* **8**(11), 1675–1675, 42 (1990).

115 Atkins G. R., Poole S. B., Sceats M. G., Simmons H. W., and Nockolds C. E., "The influence of codopants and fabrication conditions on germanium defects in optical fiber preforms," *IEEE Photon. Technol. Lett.* **4**(1), 43–46 (1992).